

High-Order Symmetric Positive Interior Quadrature Rules on Two and Three Dimensional Domains

Moustapha Diallo^{a,*}, Zelalem Arega Worku^a

^a*University of Waterloo, Department of Applied Mathematics, 200 University Avenue West, Waterloo, N2L 3G1, ON, Canada*

Abstract

Fully symmetric positive interior (f-SPI) quadrature rules are key building blocks for high-order discretizations of partial differential equations, yet high-degree rules with few nodes remain scarce on reference elements commonly used in mesh generation. We construct new f-SPI rules on the square, cube, prism, and pyramid by coupling a variable parameterization that enforces positivity and interiority with an efficient Levenberg–Marquardt optimization and a symmetry-aware node-reduction strategy that eliminates and collapses orbits, allowing transitions between symmetry types. The resulting rules achieve degrees up to 77 on the square, 45 on the cube, and 30 on the prism and pyramid, and for most degrees use fewer nodes than previously published f-SPI quadrature rules. Verification tests demonstrate comparable accuracy to existing rules. Complete node and weight data are also provided.

Keywords: Quadrature rule, Numerical integration, Prism and pyramid elements, Quadrilateral and hexahedral elements, Finite element method

1. Introduction

Quadrature rules are approximation tools for definite integrals. They play an important role in the process of solving partial differential equations (PDEs) numerically. For example, they are heavily used in discontinuous Galerkin (DG) finite element methods [1, 2, 3] and summation-by-parts

*Corresponding author.

Email addresses: mdiallo@uwaterloo.ca (Moustapha Diallo), zelalem.worku@uwaterloo.ca (Zelalem Arega Worku)

(SBP) discretizations [4, 5, 6]. The mathematical properties of such numerical methods, e.g., accuracy and stability, are affected by the type of quadrature rule used. In particular, high-degree fully symmetric, positive, and interior (f-SPI) rules with minimal nodes are often sought to obtain more accurate, stable, and efficient (speed and memory) numerical methods. The degree of available quadrature rules can also be a limiting factor on the order of numerical methods. In the case of DG methods, a degree q method can require a quadrature rule of degree up to $6q$ [7, 8, 9]. The construction of very high order f-SPI rules is thus a critical endeavor. Triangles, quadrilaterals, tetrahedra, pyramids, prisms, and hexahedra often arise as discretization elements in the application of numerical methods. For triangles and tetrahedra, there exist very high order f-SPI quadrature rules with relatively few nodes, e.g., see [10, 11, 12]; hence, our work focuses on the other four domains.

The construction of quadrature rules consists of two main steps. The first step is initialization of the rule where a distribution of nodes and weights is chosen. Several strategies have been explored in previous work, including simulated [13], particle swarm optimization [14], random distribution [15, 12, 16], tensor-product [17, 18, 10], and the use of Padua points [19]. The second step is refinement of the rule where a solver is used to find optimal distributions of nodes and weights. Commonly used techniques include Newton's method [18, 19, 12, 16, 17, 13] and the Levenberg-Marquardt algorithm (LMA) [10, 15, 20], often with some modifications to enforce domain constraints. Nodes are also added or removed at this stage. With random initializations, the intent usually is to start with a minimal node quadrature rule, but this is sometimes too ambitious and additional nodes are needed to satisfy the moment equations. In contrast, tensor-product initializations, which can easily satisfy the moment equations, lead to more nodes than necessary, requiring the removal of a relatively large number of nodes to reduce node count. The best results (in terms of degree and node count) we found on the cube, prism, and pyramid go up to degree 21, 20, and 20, respectively [12, 16]. They were constructed using node addition followed by node elimination. Similarly, the best results we can find for the square go up to degree 21 [15].

Our work builds on the methods and results from [10], where a combination of tensor-product-based initialization and node elimination is used to build very high order quadrature rules on the triangle (up to degree 84) and tetrahedron (up to degree 40). In this work, we introduce two new ways of initializing quadrature rules on the pyramid with relatively few nodes, one of

which uses results from [10]. We also present an improvement on the node elimination approach for symmetric rules, and implement a variable parameterization that turns the quadrature moment problem into an unconstrained optimization problem, enabling the use of the LMA without constraints. As a result, we push the attainable degrees upward while reducing node counts relative to existing results, obtaining rules up to degree 77, 45, 30, and 30 for the square (quadrilateral), cube (hexahedron), prism, and pyramid, respectively.

The paper is structured as follows. Section 2 defines the problem of finding a degree q quadrature rule, and Section 3 presents the solver used. Sections 4 and 5 explain the construction of initial quadrature rules and the node elimination process, respectively. Finally, Section 6 details the results, which are followed by the conclusions in Section 7.

2. Problem

An f-SPI quadrature rule of degree q in a domain D is a set of nodes and weights $Q = \{(\mathbf{x}_j, w_j) : \mathbf{x}_j \in D, w_j \in (0, \infty), j = 1, 2, \dots, n\}$ used to approximate integrals over D . The nodes are fully symmetrically distributed within the domain, and the approximation is exact for all polynomials of degree at most q , P_q ; that is,

$$\int_D f(\mathbf{x}) d\mathbf{x} = \sum_{j=1}^n w_j f(\mathbf{x}_j), \quad \forall f \in P_q. \quad (1)$$

Our domains of interest are defined as follows:

- Square (quadrilateral): $sqr = \{(x, y) \mid |x|, |y| < 1\}$,
- Cube (hexahedron): $cube = \{(x, y, z) \mid |x|, |y|, |z| < 1\}$,
- Prism: $pri = \{(x, y, z) \mid -1 < y < -x < 1, |z| < 1\}$,
- Pyramid: $pyr = \{(x, y, z) \mid |z| < 1, |x|, |y| < (1 - z)/2\}$,

which are also shown pictorially in Figure 1.

Suppose P_q is spanned by the basis $B_q = \{p_i \mid p_i \in P_q, i = 1, 2, \dots, m\}$, then the problem of finding a degree q quadrature rule over the domain D can be formulated as the following minimization problem:

$$\min_{\{\mathbf{x}_j, w_j\}_{j=1}^n} \|\mathbf{f} - V^T \mathbf{w}\|_2 \quad \text{s.t.} \quad \mathbf{x}_j \in D, \quad w_j > 0, \quad j = 1, \dots, n, \quad (2)$$

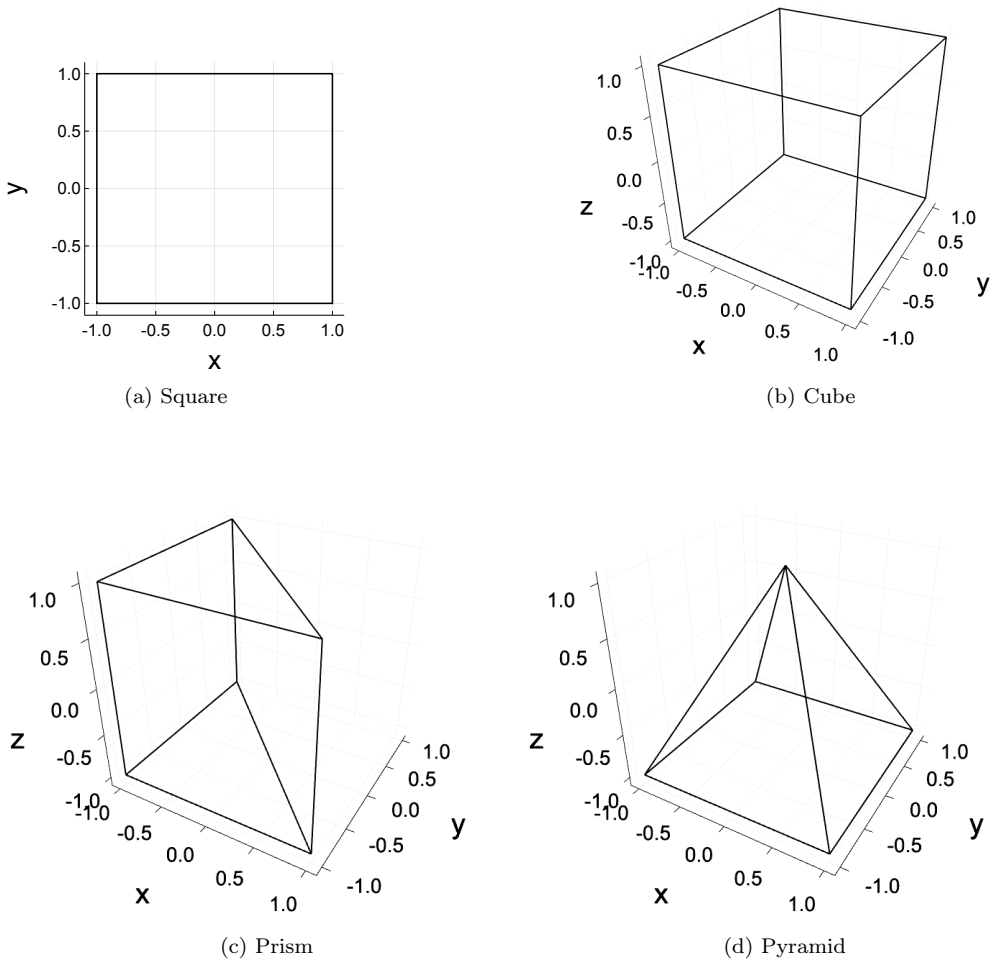


Figure 1: Visual of the domains.

where $f_i = \int_D p_i(\mathbf{x}) d\mathbf{x}$ and $V_{ji} = p_i(\mathbf{x}_j)$ for all $i = 1, \dots, m$ and $j = 1, \dots, n$. We use an orthogonal polynomial basis to obtain a well-conditioned Vandermonde matrix, V , and an easy to compute vector of the exact polynomial integrals ($f_i = \delta_{i1} * \text{constant}$). In theory, the optimality condition of the problem is that the objective is zero, but we terminate when $\|\mathbf{f} - V^T \mathbf{w}\|_2 < 10^{-66}$.

There are computational advantages to solving (2) for fully symmetric quadrature rules. First, the number of degrees of freedom can be significantly

Table 1: Pairs of (symmetry, symmetry size) grouped by the number of parameters in the symmetries.

	0-param	1-param	2-param	3-param
Square	$(S_1, 1)$	$(S_2, 4)$ $(S_3, 4)$	$(S_4, 8)$	
Cube	$(S_1, 1)$	$(S_2, 6)$, $(S_3, 8)$, $(S_4, 12)$	$(S_5, 24)$, $(S_6, 24)$	$(S_7, 48)$
Prism	$(S_1, 1)$	$(S_2, 2)$, $(S_3, 3)$	$(S_4, 6)$, $(S_5, 6)$	$(S_6, 12)$
Pyramid		$(S_1, 1)$	$(S_2, 4)$, $(S_3, 4)$	$(S_4, 8)$

smaller than the number of node coordinates. A symmetric distribution leads to dependent nodes of the same weight. Such a collection of nodes can be compressed into an orbit parameterized by a representative node and weight. Orbits are classified into different symmetries based on the number and relationship of nodes. The number of nodes associated with each orbit in a symmetry represents the size of that symmetry. Table 1 displays pairs of (symmetry, symmetry size) for each domain, grouped by the number of parameters in the symmetries. Second, symmetry implies that many moment conditions are satisfied automatically. For example, symmetric quadratures on the square exactly integrate any polynomial that is odd in at least one of the variables. Those polynomials can be removed from the orthogonal basis to reduce the number of columns of the Vandermonde matrix. The resulting set of polynomials is called an objective basis. More details on the symmetries and the objective bases used can be found in [15].

3. Levenberg-Marquardt Algorithm

We use the LMA to solve the minimization problem stated in (2). Similar to Newton's method, the LMA starts with an initial state (of the variables) $\mathbf{v}^{(0)}$ and generates a sequence of states, $\mathbf{v}^{(k)}$,

$$\mathbf{v}^{(k+1)} = \mathbf{v}^{(k)} + \mathbf{d}\mathbf{v}^{(k)}, \quad (3)$$

that ideally converges to a global minimum of the problem. There are several variants of the algorithm, and we use the one described in [10]. The LMA is designed for unconstrained optimization problems, but (2) has constraints — interior nodes and positive weights. We explored two ways of addressing this issue.

The first approach consists of using a Cartesian parameterization of the variables and projection of $\mathbf{v}^{(k+1)}$ inside the domain. We perform the projection through scaling down $\mathbf{d}\mathbf{v}^{(k)}$ by the largest scaling factor $\alpha \in (0, 1]$ that

ensures $\mathbf{v}^{(k+1)}$ lies within the domain. This scalar is computed as follows:

$$\alpha = \min \{\alpha_i : i = 1, \dots, n_v\},$$

$$\alpha_i = \begin{cases} \frac{v_i^{(k)} + dv_i^{(k)} - (v_{i,\min} + \epsilon_m)}{dv_i^{(k)}}, & \text{if } v_i^{(k)} + dv_i^{(k)} \leq v_{i,\min} \\ \frac{v_i^{(k)} + dv_i^{(k)} - (v_{i,\max} - \epsilon_m)}{dv_i^{(k)}}, & \text{if } v_i^{(k)} + dv_i^{(k)} \geq v_{i,\max} \\ 1, & \text{otherwise,} \end{cases} \quad (4)$$

where n_v is the number of variables, $(v_{i,\min}, v_{i,\max})$ is the domain of variable v_i , and ϵ_m is the machine precision for the number type being used, `Float64` or `BigFloat`. Coordinate variables are normalized so that their domain is $(0, 1)$, and weight variables have domain $(0, \infty)$. A similar projection method is used in [10].

The second approach reformulates (2) as an unconstrained optimization problem using exponential parameterization of the variables. This reparameterization is particularly useful because it enforces positivity and interiority by construction. For a variable with Cartesian parameter $x \in (0, 1)$, we use the exponential parameter $z \in \mathbb{R}$ given by the following:

$$x = \frac{1}{1 + e^{-sz}}, \quad s = 0.01. \quad (5)$$

For a variable with Cartesian parameter $x \in (0, \infty)$, we use the exponential parameter $z \in \mathbb{R}$ given by the following:

$$x = e^{sz}. \quad (6)$$

We experimented with several values for s and selected $s = 0.01$, which consistently led to the elimination of the largest number of nodes.

Exponential parameterization is computationally faster because it avoids repeated projections, but it is more prone to numerical instabilities, often resulting in ill-conditioned or singular matrices in the LMA update. To balance robustness and efficiency, we employ a hybrid strategy: exponential parameterization is used by default, and the solver reverts locally to Cartesian parameters whenever an inversion failure is detected.

4. Initial Quadrature Construction

The first step of our approach is to construct the initial quadrature rules. At this stage, the goal is to make quadrature rules that have few nodes

without being too restrictive, e.g. having no nodes on some symmetries. We mainly construct them by decomposing the domains into lower-dimensional components and using the best known quadratures on those components.

Suppose that we are constructing a degree q quadrature rule, and let $p_q(\mathbf{x})$ be an arbitrary polynomial of degree at most q . We present the approach for each domain considered.

4.1. Square

The square can be viewed as the tensor-product of two line segments on $(-1, 1)$:

$$\begin{aligned} \int_{sqr} p_q(\mathbf{x}) d\mathbf{x} &= \int_{-1}^1 \left(\int_{-1}^1 p_q(\mathbf{x}) dx \right) dy \\ &= \int_{-1}^1 \sum_{a=1}^A w_{la} p_q(x_{la}, y) dy \\ &= \sum_{a=1}^A \sum_{b=1}^A w_{la} w_{lb} p_q(x_{la}, x_{lb}), \end{aligned}$$

where $\{(x_{la}, w_{la}) \mid a = 1, \dots, A\}$ is the Gauss-Legendre quadrature rule on $(-1, 1)$ of degree at least q with the minimal odd number of nodes. The resulting quadrature on the square is $\{(x_{la}, x_{lb}, w_{la} w_{lb}) \mid a, b = 1, \dots, A\}$. The choice of Gauss-Legendre quadratures with an odd number of nodes ensures that the initial quadrature has nodes on the S_1 and S_2 symmetries.

4.2. Cube

The cube can be viewed as the tensor-product of three line segments on $(-1, 1)$:

$$\begin{aligned} \int_{cube} p_q(\mathbf{x}) d\mathbf{x} &= \int_{-1}^1 \left(\int_{-1}^1 \left(\int_{-1}^1 p_q(\mathbf{x}) dx \right) dy \right) dz \\ &= \int_{-1}^1 \left(\int_{-1}^1 \sum_{a=1}^A w_{la} p_q(x_{la}, y, z) dy \right) dz \\ &= \int_{-1}^1 \sum_{a=1}^A \sum_{b=1}^A w_{la} w_{lb} p_q(x_{la}, x_{lb}, z) dz \\ &= \sum_{a=1}^A \sum_{b=1}^A \sum_{c=1}^A w_{la} w_{lb} w_{lc} p_q(x_{la}, x_{lb}, x_{lc}). \end{aligned}$$

The resulting quadrature on the cube is $\{(x_{la}, x_{lb}, x_{lc}, w_{la}w_{lb}w_{lc}) \mid a, b, c = 1, \dots, A\}$. Here, the use of an odd degree Legendre-Gauss quadrature rule on $(-1, 1)$ ensures that the cube has nodes on its S_1 , S_2 , S_4 , and S_5 symmetries.

4.3. Prism

The prism can be viewed as the tensor-product of the line segment $(-1, 1)$ and the triangle $tri = \{(x, y) \mid -1 < y < -x < 1\}$:

$$\begin{aligned} \int_{pri} p_q(\mathbf{x}) d\mathbf{x} &= \int_{-1}^1 \left(\int_{tri} p_q(\mathbf{x}) dx dy \right) dz \\ &= \int_{-1}^1 \sum_{b=1}^B w_{tb} p_q(x_{tb}, y_{tb}, z) dz \\ &= \sum_{b=1}^B \sum_{a=1}^A w_{tb} w_{la} p_q(x_{tb}, y_{tb}, x_{la}), \end{aligned}$$

where $\{(x_{tb}, y_{tb}, w_{tb}) \mid b = 1, \dots, B\}$ is the degree q f-SPI quadrature rule presented in [10] for the triangle. We add the centroid whenever absent to ensure that initial quadrature rules have nodes on the S_1 and S_2 symmetries. The resulting quadrature rule on the prism is $\{(x_{tr}, y_{tr}, x_{ls}, w_{tr}w_{ls}) \mid r = 1, \dots, b, s = 1, \dots, a\}$.

4.4. Pyramid

We developed two ways of initializing the pyramid. One uses an algebraic construction while the other uses a geometric construction. The algebraic construction consists of expressing integration over the pyramid as a composition of an integral over $(-1, 1)$ and an integral over $(-1, 1)^2$:

$$\begin{aligned} \int_{pyr} p_q(\mathbf{x}) d\mathbf{x} &= \int_{-1}^1 \left(\int_{-\alpha_z}^{\alpha_z} \int_{-\alpha_z}^{\alpha_z} p_q(x, y, z) dx dy \right) dz \\ &= \int_{-1}^1 \left(\alpha_z^2 \int_{-1}^1 \int_{-1}^1 p_q(\alpha_z x, \alpha_z y, z) dx dy \right) dz \\ &= \int_{-1}^1 \alpha_z^2 \sum_{c=1}^C w_{sc} p_q(\alpha_z x_{sc}, \alpha_z y_{sc}, z) dz \\ &= \sum_{e=1}^E \sum_{c=1}^C \alpha_{x_{le}}^2 w_{sc} w_{le} p_q(\alpha_{x_{le}} x_{sc}, \alpha_{x_{le}} y_{sc}, x_{le}), \end{aligned}$$

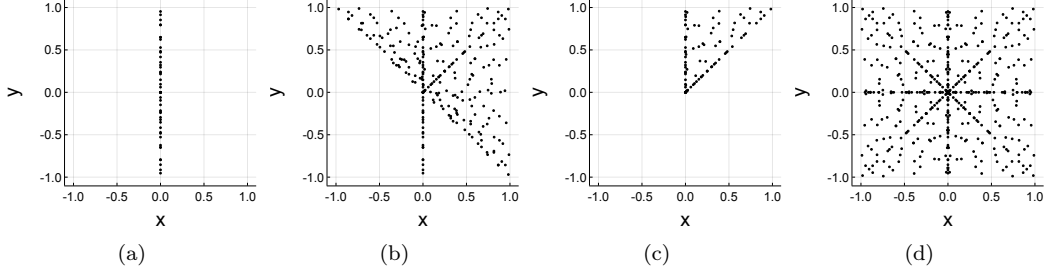


Figure 2: Base view of the geometric construction of a degree 15 quadrature rule on the pyramid.

where $\alpha_z = (1 - z)/2$, $\{(x_{le}, w_{le}) \mid e = 1, \dots, E\}$ is the degree $q + 2$ Gauss-Legendre quadrature rule on $(-1, 1)$, and $\{(x_{sc}, y_{sc}, w_{sc}) \mid c = 1, \dots, C\}$ is our best result for degree q on the square with the center included to ensure that the initial quadrature on the pyramid has nodes on the S_1 symmetry. The resulting quadrature rule on the pyramid is $\{(\alpha_{x_{le}} x_{sc}, \alpha_{x_{le}} y_{sc}, x_{le}, \alpha_{x_{le}}^2 w_{sc} w_{le}) \mid c = 1, \dots, C, e = 1, \dots, E\}$.

The geometric construction splits the pyramid into triangles and tetrahedra. The steps involved are:

- (a) map the nodes of the degree q triangular quadrature rule from [10] to $\{(0, y, z) \mid |z| < 1, |y| < (1 - z)/2\} \subset \text{pyr}$;
- (b) map the nodes of the degree $q - 2$ tetrahedral quadrature rule from [10] to $\{(x, y, z) \mid |z| < 1, |x|, |y| < (1 - z)/2, -x < y\} \subset \text{pyr}$;
- (c) remove the nodes not in $\{(x, y, z) \mid 0 \leq x \leq y < 1 \mid z \mid < 1\}$;
- (d) use the symmetries of the pyramid to generate more nodes;
- (e) set each weight to (pyramid volume)/(node count), then pass the quadrature rule to the LMA.

Figure 2 provides a visual of steps (a) to (d) for the geometric construction of a degree 15 quadrature rule on the pyramid.

It appears that the only previously used method to make a convergent quadrature rule, without using an optimization algorithm, on the pyramid is through a Duffy transformation [21]. It works by mapping an integral over the pyramid to an integral over the cube but leads to a quadrature rule with a very high number of nodes as a degree q rule on the pyramid requires a

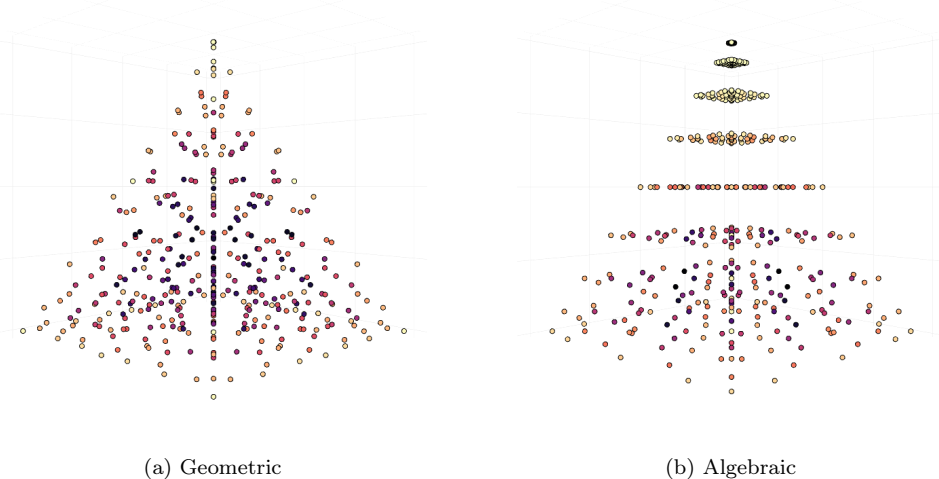


Figure 3: Geometric and algebraic initializations for degree 15 quadrature rule on the pyramid with darker nodes having larger weight values.

degree $2q + 2$ rule on the cube. The algebraic construction described above is also convergent without optimization; however, it only requires a degree q rule on the square and a degree $q + 2$ Gauss-Legendre rule, which results in a significantly lower node count compared to the Duffy construction. For instance, a degree 15 quadrature rule on the pyramid has 1787 and 441 nodes with the Duffy and algebraic constructions, respectively. The Duffy transformation in this case uses the degree 33 quadrature rule we have obtained on the cube to produce the quadrature rule on the pyramid with 1787 nodes.

Unlike the algebraic construction, the geometric one does not automatically satisfy the moment equations. Optimization is required to get a quadrature rule using the geometric construction, but a relatively low number of LMA iterations suffices. Nevertheless, it yields significantly fewer and more evenly distributed nodes, as can be seen in Figure 3. Furthermore, the gap in node count between the two constructions increases with the quadrature degree. For degree 30, the geometric construction has 572 fewer nodes than the algebraic one.

5. Node Elimination

Once an initial quadrature is constructed, the next step is to reduce the number of nodes as much as possible. Our approach combines orbit elimination and orbit collapse. The elimination of an orbit is the removal of the nodes associated with it. A critical aspect of this part is the order of elimination attempts, as it affects the number of nodes that can be removed. Our strategy is inspired by the one described in [10] for the triangle and tetrahedron, which removes orbits strictly from larger symmetries first, then within each symmetry, removes orbits with smallest weights first. We also remove orbits in this order, but symmetries sharing the same number of parameters are bundled and relatively prioritized by assigning them priority numbers. Consider an orbit of Cartesian weight w_C and exponential weight w_e that is part of a d -parameter symmetry with priority number $p \geq 1$. The orbit's priority relative to other orbits in a d -parameter symmetry is set to $p_C = p \times w_C$ under Cartesian parameterization and $p_e = p' + w_e$ under exponential parameterization, where $p' = \log(p)/s$. This setup ensures consistent prioritization under parameterization changes. Indeed, $p_C = e^{s p_e}$ because $w_C = e^{s w_e}$ via (6), so $p_{C1} < p_{C2} \iff p_{e1} < p_{e2}$. Each domain has a pair of symmetries of the same size and the same number of parameters (see Table 1), and we experimented with assigning those symmetries the same relative priority. However, prioritizing S_2 over S_3 on the square and pyramid, S_5 over S_6 on the cube, and S_5 over S_4 on the prism leads to the elimination of more nodes than otherwise. Table 2 shows which symmetries are bundled (relatively prioritized) and the relative priorities within each bundle, and Algorithm 1 outlines how orbit elimination works on a bundle of symmetries.

The collapse of an orbit is its replacement by another orbit in a symmetry with fewer parameters. The sizes of symmetries decrease with the number of parameters, so a collapse reduces the number of nodes in a quadrature rule. Consider an orbit O_i of weight w in a d -parameter symmetry S_i . We attempt to collapse the orbit onto $(d - 1)$ -parameter symmetries within a prescribed geometric distance, which is referred to as the collapse threshold and denoted by \mathcal{CT} . Each symmetry of a domain corresponds to a region in it, hence the use of the term distance. Suppose O_i is eligible for a collapse on the symmetry S_f . The replacement orbit O_f is set to be the orbit in S_f closest to O_i with weight $(|S_i|/|S_f|) \times w$, where $|S_i|$ and $|S_f|$ are the sizes of S_i and S_f , respectively. The total weight of the nodes associated with O_i is the same as the total weight of the ones associated with O_f . In case O_f can be collapsed

Table 2: Symmetry bundles \mathcal{SB} and corresponding priority bundles \mathcal{PB} .

square	$\mathcal{SB} = [[S_4], [S_3, S_2], [S_1]]$ $\mathcal{PB} = [[1], [10^5, 1], [1]]$
cube	$\mathcal{SB} = [[S_7], [S_6, S_5], [S_4, S_3, S_2], [S_1]]$ $\mathcal{PB} = [[1], [10^5, 1], [1, 10^5, 10^{10}], [1]]$
prism	$\mathcal{SB} = [[S_6], [S_5, S_4], [S_3, S_2], [S_1]]$ $\mathcal{PB} = [[1], [1, 10^5], [1, 10^5], [1]]$
pyramid	$\mathcal{SB} = [[S_4], [S_3, S_2], [S_1]]$ $\mathcal{PB} = [[1], [10^5, 1], [1]]$

on multiple symmetries, we first attempt the collapse on symmetries with lower priority numbers, targeting smallest size symmetries to maximize node elimination. The collapse threshold is set to $\mathcal{CT} = 0.25$ for degrees below 31 on the square and below 20 on 3D domains where nodes are sparse. It is set to 0.1 for higher degrees, where nodes are denser. Algorithm 2 describes how orbit elimination and collapse are combined.

Orbit collapse makes the node elimination process more robust by allowing a flow of orbits between symmetries. Suppose that the minimal node quadrature rule of degree q for some domain has 5 orbits on its S_k symmetry, but the initial quadrature rule only has 2 orbits on S_k . In this case, the initialization must have extra orbits on other symmetries since it is not minimal. Orbit elimination alone cannot lead to the minimal number of nodes, but with orbit collapse, it is possible to get there because S_k can take orbits from other symmetries.

An important part of the node elimination process is the stopping criteria of the LMA iteration. It depends on two parameters: the convergence check interval, C_I , and the maximum iteration, M_I . After $C_I \times k$ iterations, $k \in \mathbb{N}$, the algorithm checks whether the residual is less than the initial residual divided by 10^k and stops if that is not the case. This setup helps avoid wasting hundreds of iterations on orbits that cannot be eliminated. The algorithm also stops after M_I iterations. C_I is set to values between 20 and 70, increasing it with the number of variables, and M_I is set to 500.

Algorithm 1 Procedure for eliminating orbits of a quadrature \mathcal{Q} with degree q from a set of symmetries \mathcal{S} with corresponding priority numbers in \mathcal{P} .

```

1: procedure REMOVEORBITS( $\mathcal{Q}, q, \mathcal{S}, \mathcal{P}$ )
2:   OrbitPriorities  $\leftarrow$  COMPUTEORBITPRIORITIES( $\mathcal{Q}, q, \mathcal{S}, \mathcal{P}$ )
3:    $i \leftarrow 0$  ▷ number of explored orbits
4:   while  $i < \#\text{orbits from } \mathcal{S}$  do
5:     if  $\mathcal{Q}$  has a single orbit then
6:       break
7:     end if
8:     TargetOrbit  $\leftarrow$  orbit with  $i$ th smallest priority
9:      $\mathcal{Q}' \leftarrow$  a copy of  $\mathcal{Q}$  with Target removed
10:    Residual  $\leftarrow$  LMA( $\mathcal{Q}', q$ )
11:    if Residual  $<$  tolerance then
12:       $\mathcal{Q} \leftarrow \mathcal{Q}'$ 
13:      OrbitPriorities  $\leftarrow$  COMPUTEORBITPRIORITIES( $\mathcal{Q}, \mathcal{S}, \mathcal{P}$ )
14:       $i \leftarrow 0$ 
15:    else
16:      if Target's symmetry has been fully explored then
17:        remove it from  $\mathcal{S}$  and its priority number from  $\mathcal{P}$ 
18:      end if
19:       $i \leftarrow i + 1$  ▷ moving onto the next orbit
20:    end if
21:  end while
22: end procedure

```

6. Results

6.1. Quadrature Rules

Our algorithm has led to numerous f-SPI quadrature rules with fewer nodes than existing ones across all four domains. Tables 3, 4, 5, and 6 contain the number of nodes for each of our quadrature rules, with degrees where they are better than existing ones underlined. Existing quadrature rules have fewer nodes than presented in this work in only two instances (for degrees 7 and 9 rules on the prism), and the difference is exactly one node for each case. We only report odd degree rules on the square and cube because, similar to Legendre-Gauss rules in 1D, there are no even-degree fully symmetric quadrature rules on these domains. The nodal distributions

Algorithm 2 Procedure for eliminating nodes of a degree q quadrature \mathcal{Q} using orbit elimination and collapse given symmetry bundles \mathcal{SB} and priority bundles \mathcal{PB} , as defined in Table 2, and a collapse threshold \mathcal{CT} .

```

1: procedure REMOVENODES( $\mathcal{Q}, q, \mathcal{SB}, \mathcal{PB}, \mathcal{CT}$ )
2:   for each index  $i$  of  $\mathcal{SB}$  do                                 $\triangleright$  indexing starts at 1
3:     REMOVEORBITS( $\mathcal{Q}, q, \mathcal{SB}[i], \mathcal{PB}[i]$ )           $\triangleright$  see Algorithm 1
4:     for  $j = 1 : i$  do
5:       COLLAPSEORBITS( $\mathcal{Q}, q, \mathcal{SB}[j]$ )
6:     end for
7:   end for
8: end procedure

```

Table 3: Results for the square.

q	New	[15]	q	New	[15]	q	New	q	New	q	New
1	1	1	<u>17</u>	57	60	<u>33</u>	201	<u>49</u>	433	<u>65</u>	757
3	4	4	<u>19</u>	72	72	<u>35</u>	224	<u>51</u>	465	<u>67</u>	805
5	8	8	<u>21</u>	85	85	<u>37</u>	249	<u>53</u>	501	<u>69</u>	849
7	12	12	<u>23</u>	101		<u>39</u>	277	<u>55</u>	541	<u>71</u>	904
9	20	20	<u>25</u>	120		<u>41</u>	304	<u>57</u>	576	<u>73</u>	953
11	28	28	<u>27</u>	137		<u>43</u>	336	<u>59</u>	613	<u>75</u>	1001
13	37	37	<u>29</u>	157		<u>45</u>	365	<u>61</u>	660	<u>77</u>	1049
15	48	48	<u>31</u>	177		<u>47</u>	397	<u>63</u>	709		

Table 4: Results for the cube.

q	New	[16]	q	New	[16]	q	New	[16]	q	New	q	New
1	1	1 [15]	11	90	90	<u>21</u>	495	580	<u>31</u>	1478	<u>41</u>	3338
3	8		<u>13</u>	148	154	<u>23</u>	617		<u>33</u>	1787	<u>43</u>	3870
5	14	14	<u>15</u>	199	256	<u>25</u>	828		<u>35</u>	2102	<u>45</u>	4414
7	34	34	<u>17</u>	282	346	<u>27</u>	984		<u>37</u>	2506		
9	58	58	<u>19</u>	369	454	<u>29</u>	1258		<u>39</u>	2856		

for selected quadrature rules on the square, cube, prism, and pyramid are displayed in Figures A.14 to A.17, respectively, in Appendix A.

We quantify the efficiency of a quadrature rule for a given domain by comparing it with the best we can build using quadrature rules on lower-dimensional domains. In the case of the square, cube, and prism, the reference rules are tensor-product constructions. These coincide with our initial

Table 5: Results for the prism.

q	New	[16]	q	New	[16]	q	New	[16]	q	New	q	New
1	1	1 [15]	8	46	46	15	220	238	22	635	29	1311
2	5	5	9	60	59	16	264	287	23	695	30	1460
3	8	8	10	82	84	17	299	338	24	772		
4	11	11	11	97	99	18	359	396	25	878		
5	16	16	12	127	136	19	405	420	26	986		
6	28	28	13	146	162	20	470	518	27	1080		
7	36	35	14	182	194	21	545		28	1197		

Table 6: Results for the pyramid

q	New	[12]	q	New	[12]	q	New	[12]	q	New	q	New
1	1	1 [15]	8	44	47	15	203	234	22	595	29	1275
2	5	5	9	56	62	16	254	285	23	665	30	1417
3	6	6	10	76	80	17	293	319	24	756		
4	10	10	11	92	103	18	344	357	25	843		
5	15	15	12	120	127	19	394	418	26	942		
6	23	23	13	142	152	20	464	489	27	1050		
7	31	31	14	175	184	21	522		28	1171		

rules, except where we intentionally added extra orbits to make sure some symmetries are non-empty. For the pyramid, we use algebraic constructions as a reference without any extra orbits added. The efficiency of a degree q quadrature rule with n nodes, relative to a reference quadrature rule with n_r nodes, is defined as

$$e = \frac{n_r - n}{n_r}. \quad (7)$$

The number of reference nodes is given by

$$\left(\left\lceil \frac{q+1}{2} \right\rceil \right)^2, \left(\left\lceil \frac{q+1}{2} \right\rceil \right)^3, \\ \left(\left\lceil \frac{q+1}{2} \right\rceil \right) \times n_T(q), \text{ and } \left(\left\lceil \frac{(q+2)+1}{2} \right\rceil \right) \times n_S(q)$$

on the square, cube, prism, and pyramid, respectively, where $n_T(q)$ and $n_S(q)$ are the number of nodes of the best degree q quadrature rule on the triangle [10] and square (our results), respectively.



Figure 4: Efficiency on the square and cube.

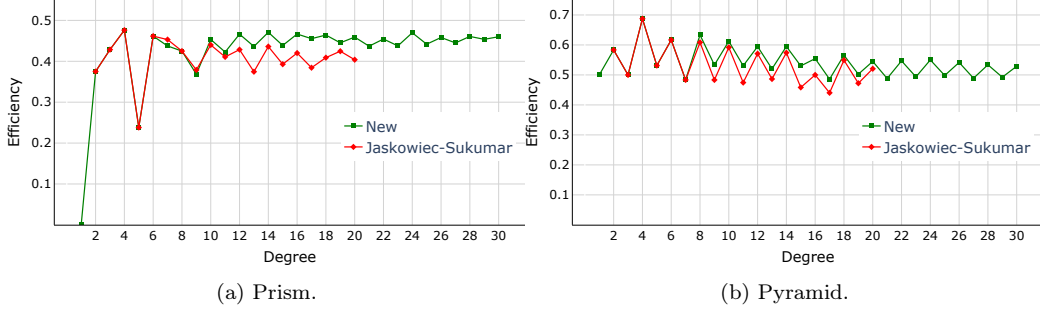


Figure 5: Efficiency on the prism and pyramid.

The significance of this metric lies not in its value at a particular degree but rather how it changes with the quadrature degree. For low degrees, the optimization problem has few variables and is easy to solve; we could conveniently explore various node reduction strategies and are thus confident that the quadrature rules obtained there have an almost minimal number of nodes. By low degrees, we mean 1-31 and 1-21 for the square and cube, respectively, and 1-14 for the prism and pyramid, because it takes a very short amount of time to go through the initialization and node elimination process. We use the efficiency trend at low degrees to make a judgment about the performance of the algorithm at high degrees.

On the square, the efficiency increases rapidly between $q = 1$ and $q = 21$, going from 0 to about 0.30, but does not change much beyond that, see Figure 4a. The efficiency at degree 77 being comparable to that of degrees 21-31 is a good indicator of a steady performance of the node elimination algorithm. There is a similar trend on the cube (prism), see Figure 4b (5a), where the efficiency reaches 0.61 (0.45) at degree 15 (10) and stays within



Figure 6: Approximation of $I(10, 15)$ with mesh of one square.

0.625 ± 0.025 (0.44 ± 0.02) all the way up to degree 45 (30). It also has a steady trend on the pyramid, see Figure 5b, but an oscillatory one, unlike the other three domains.

6.2. Numerical Experiments

The quadrature rules presented in this work are based on polynomials, but they can be used to approximate integrals of all kinds of functions. Oscillatory functions are usually a challenge, and we use them to test our results. Specifically, we use the functions

$$f(x, y) = \cos(k_1 x + k_2 y) \quad \text{and} \quad (8)$$

$$g(x, y, z) = \cos(k_1 x + k_2 y + k_3 z) \quad (9)$$

in two and three dimensions, respectively, where k_1 , k_2 , and k_3 are whole numbers. We proceed by approximating the integral

$$I(k_1, k_2) = \int_{-1}^1 \int_{-1}^1 f(x, y) dx dy = \frac{4 \sin(k_1) \sin(k_2)}{k_1 k_2} \quad (10)$$

using quadrature rules on a mesh of squares and approximating the integral

$$I(k_1, k_2, k_3) = \int_{-1}^1 \int_{-1}^1 \int_{-1}^1 g(x, y, z) dx dy dz = \frac{8 \sin(k_1) \sin(k_2) \sin(k_3)}{k_1 k_2 k_3} \quad (11)$$

using quadrature rules on a mesh of cubes, prisms, and pyramids.

Figures 6, 7, 8, and 9 show that the absolute errors in the approximations of $I(k_1, k_2)$ and $I(k_1, k_2, k_3)$ using our quadrature rules decrease as the quadrature degree increases — at rates comparable to those of existing quadrature rules. In addition, Figures 10, 11, 12, and 13 display a convergence rate of at least $q + 1$ for a degree q quadrature rule with mesh refinement. The convergence rate is close to $q + 2$ for even degrees, and similar observations were made in [10] for the tetrahedra.

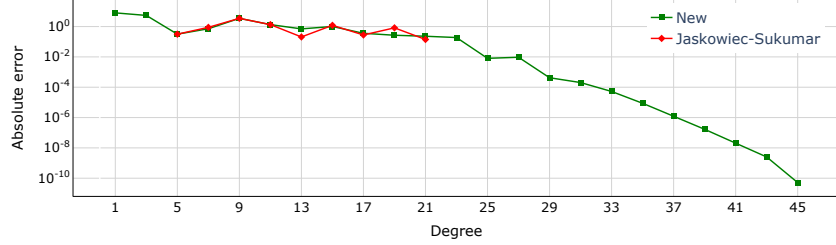


Figure 7: Approximation of $I(5, 5, 15)$ with mesh of one cube.

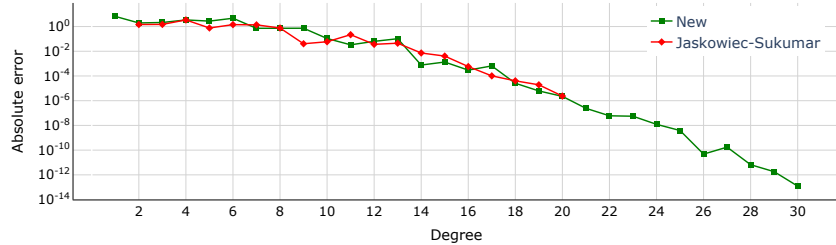


Figure 8: Approximation of $I(1, 1, 10)$ with mesh of two prisms.

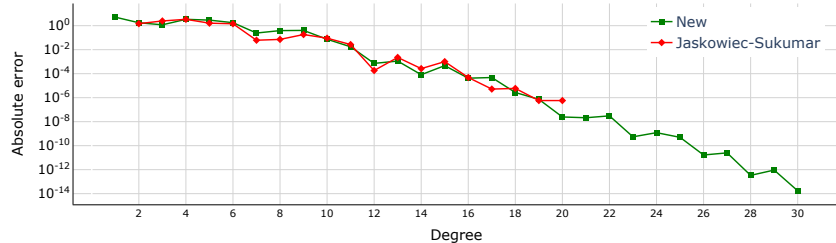


Figure 9: Approximation of $I(1, 1, 10)$ with mesh of six pyramids.

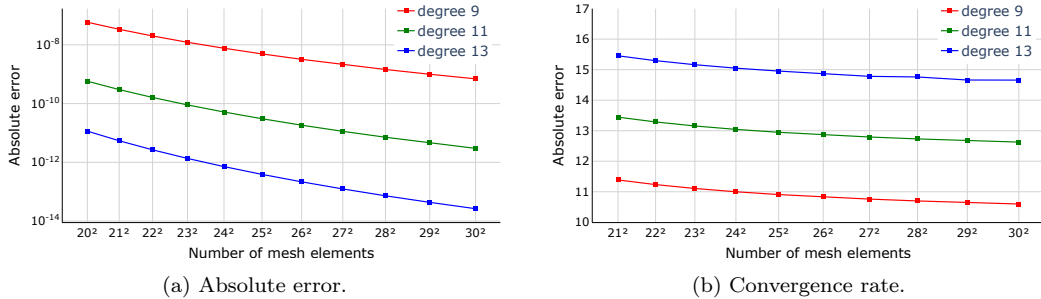


Figure 10: Approximation of $I(30, 30)$ with meshes of squares of various number of elements.

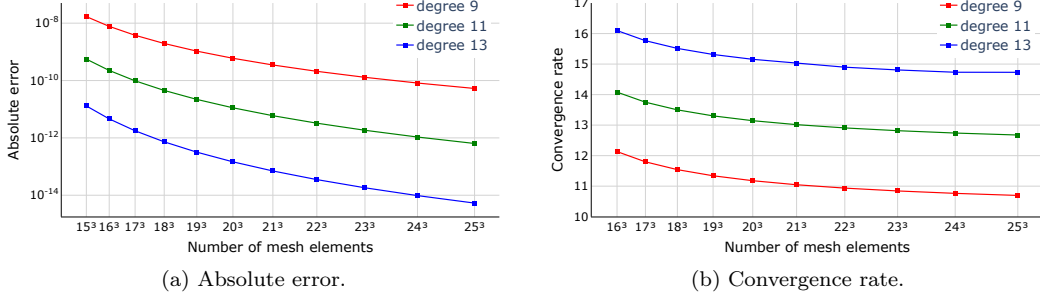


Figure 11: Approximation of $I(30, 10, 20)$ with meshes of cubes of various number of elements.

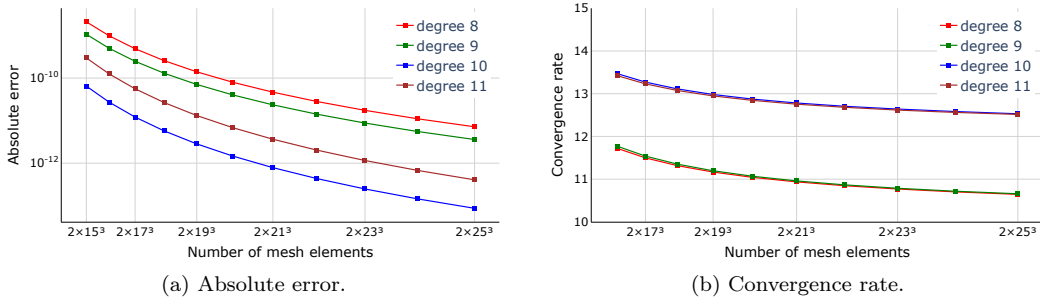


Figure 12: Approximation of $I(40, 20, 20)$ with meshes of prisms of various number of elements.

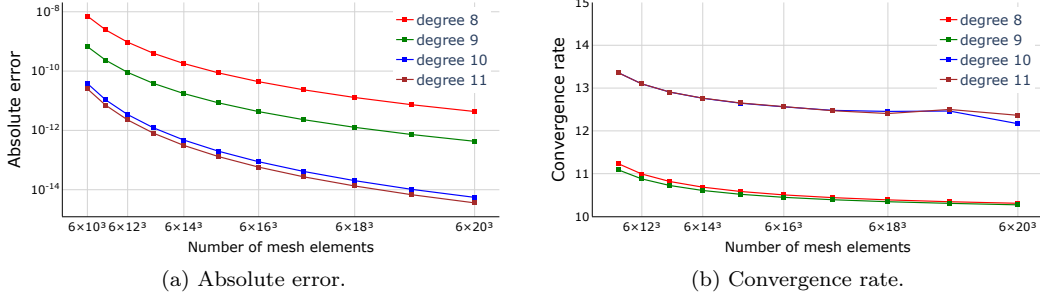


Figure 13: Approximation of $I(15, 5, 15)$ with meshes of pyramids of various number of elements.

7. Conclusions

In this work, we developed a practical framework for constructing f-SPI quadrature rules on commonly used multidimensional reference elements. The approach combines a variable parameterization that enforces positiv-

ity and interiority with a Levenberg–Marquardt optimization algorithm and a symmetry-aware node-reduction strategy based on orbit elimination and orbit collapse. Orbit collapse, in particular, improves robustness by allowing orbits to transition between symmetry types, enabling node reduction beyond what orbit elimination alone typically permits. Using these ingredients, we produced new f-SPI quadrature rules on the square, cube, prism, and pyramid. The resulting rules reach degrees up to 77 on the square, 45 on the cube, and 30 on the prism and pyramid, and for most degrees we obtain improved node counts relative to previously published f-SPI rules. Numerical experiments confirm the expected convergence behavior and demonstrate accuracy comparable to existing rules. Complete node and weight data are provided to facilitate direct use in high-order discretizations of PDEs. Several directions for future work remain open. Further improvements in initialization strategies and solver robustness could extend the attainable degrees in three dimensions and reduce node counts further. Extending the approach to construct quadrature rules with nodes on element boundaries is also of interest, as such rules enable efficient entropy-stable discretizations within the summation-by-parts framework.

Appendix A. Nodal Distributions of Selected Quadrature Rules

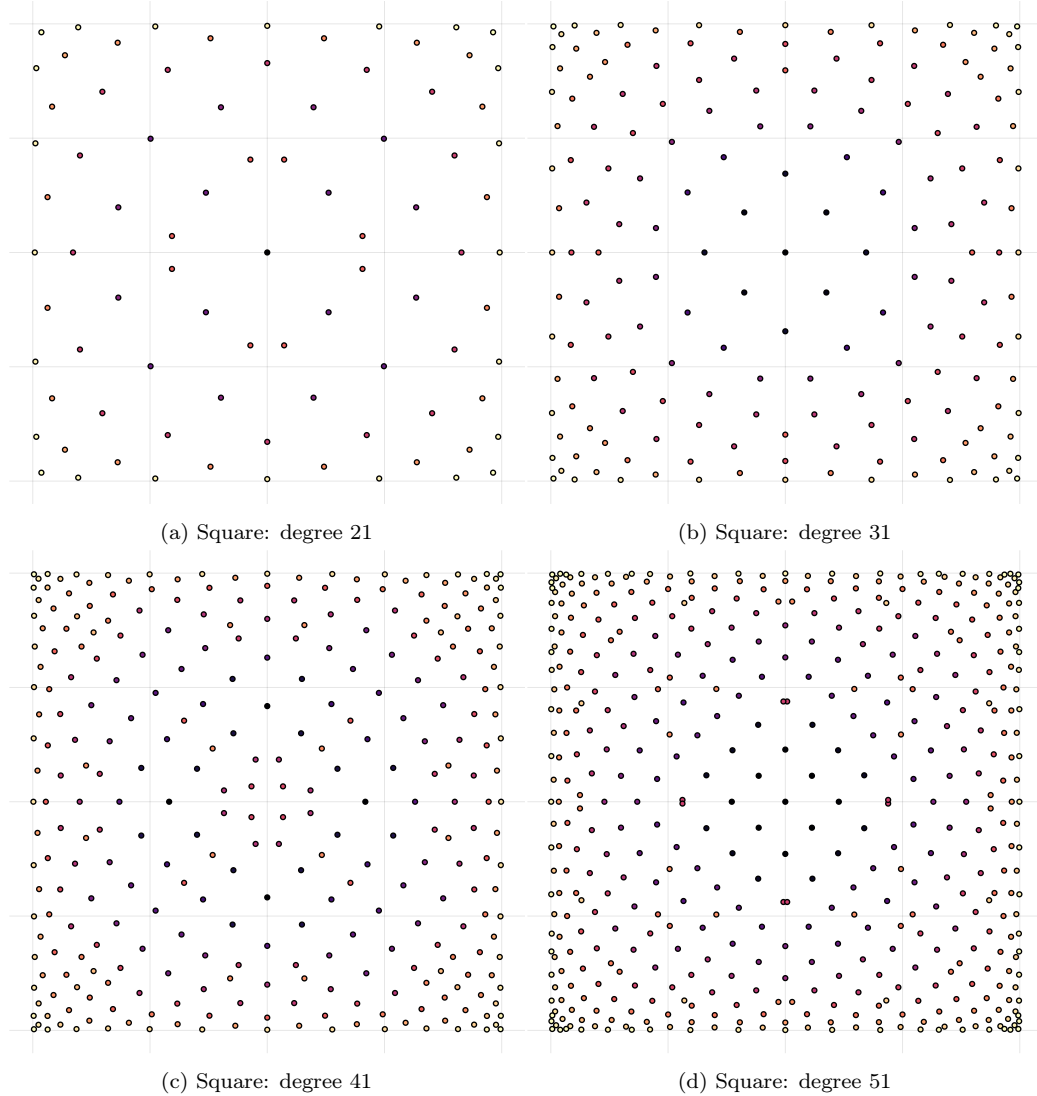
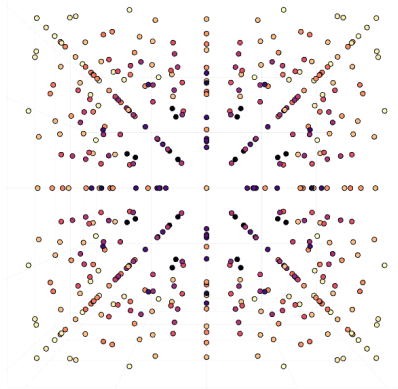
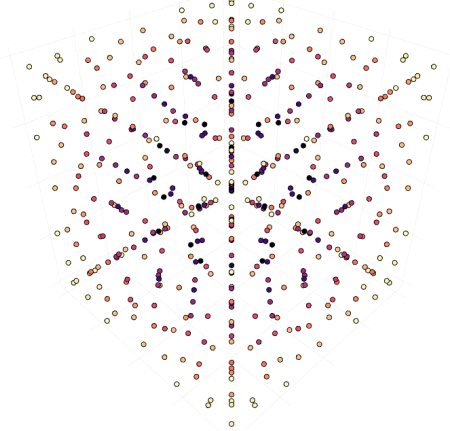


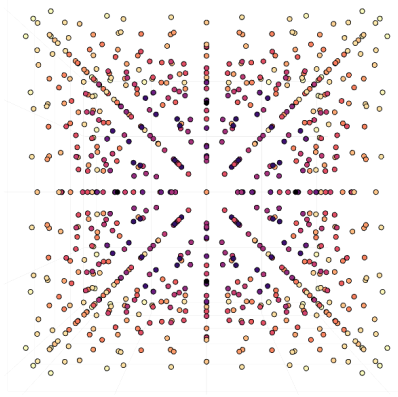
Figure A.14: Final quadrature rules obtained on the square for degrees 21, 31, 41, and 51; darker nodes have more weight.



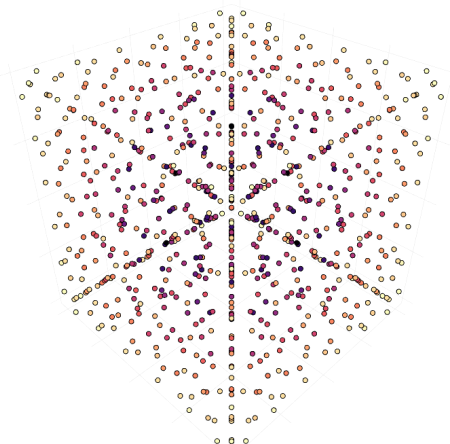
(a) Cube: degree 21



(b) Cube: degree 21

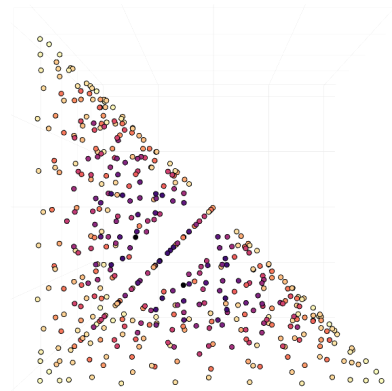


(c) Cube: degree 25

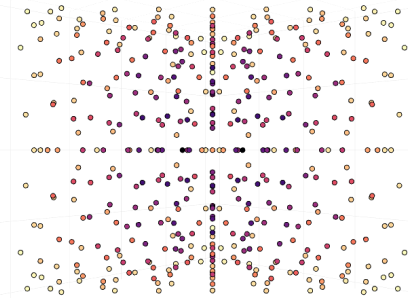


(d) Cube: degree 25

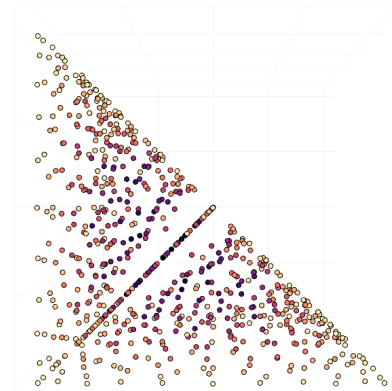
Figure A.15: Final quadrature rules obtained on the cube for degrees 21 and 25, with a face view (left) and a diagonal view (right); darker nodes have more weight.



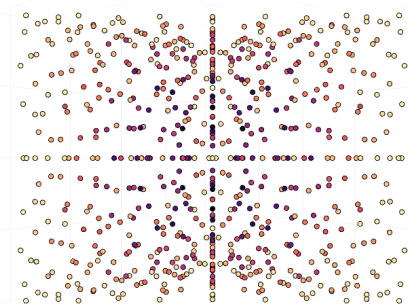
(a) Prism: degree 20



(b) Prism: degree 20

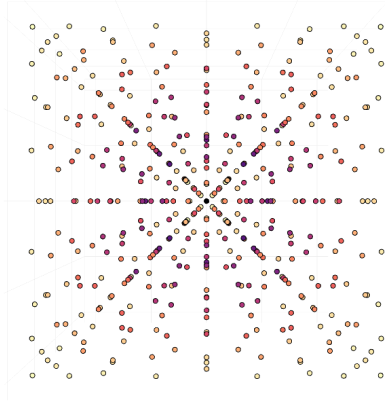


(c) Prism: degree 23

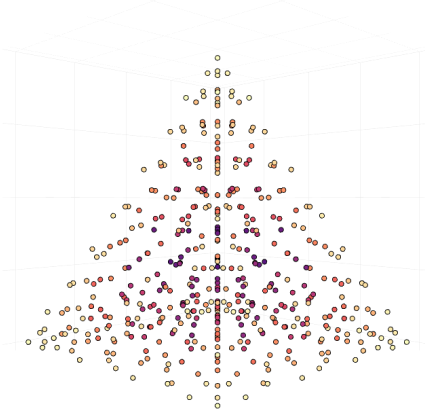


(d) Prism: degree 23

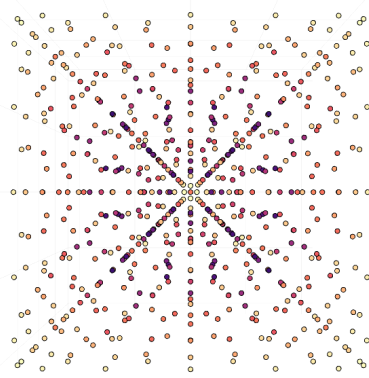
Figure A.16: Final quadrature rules obtained on the prism for degrees 20 and 23 with a top view (left) and a diagonal view (right); darker nodes have more weight.



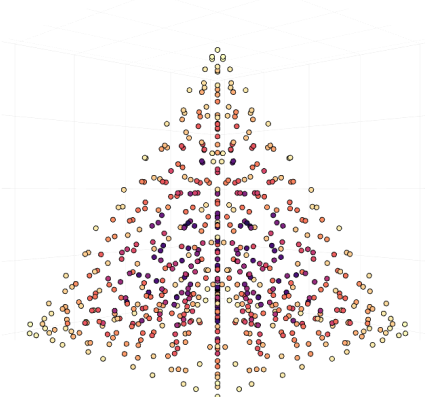
(a) Pyramid: degree 20



(b) Pyramid: degree 20



(c) Pyramid: degree 23



(d) Pyramid: degree 23

Figure A.17: Final quadrature rules obtained on the pyramid for degrees 20 and 23 with a base view (left) and a side view (right); darker nodes have more weight.

Appendix B. Supplementary Materials

The nodal and weight data of the quadrature rules derived in this work can be found at <https://github.com/mdiallo-fula/SymmetricPositiveInteriorCubatures.jl/tree/master/data/published-results>.

References

- [1] W. H. Reed, T. R. Hill, Triangular mesh methods for the neutron transport equation, Los Alamos Scientific Lab., N.Mex. (USA), 1973.
- [2] B. Cockburn, C.-W. Shu, The Runge–Kutta discontinuous Galerkin method for conservation laws v: Multidimensional systems, *Journal of Computational Physics* 141 (2) (1998) 199–224.
- [3] J. S. Hesthaven, T. Warburton, *Nodal discontinuous Galerkin methods: algorithms, analysis, and applications*, Springer, 2008.
- [4] D. C. Del Rey Fernández, J. E. Hicken, D. W. Zingg, Review of summation-by-parts operators with simultaneous approximation terms for the numerical solution of partial differential equations, *Computers & Fluids* 95 (2014) 171–196.
- [5] M. Svärd, J. Nordström, Review of summation-by-parts schemes for initial–boundary-value problems, *Journal of Computational Physics* 268 (2014) 17–38.
- [6] J. E. Hicken, D. C. Del Rey Fernández, D. W. Zingg, Multidimensional summation-by-parts operators: General theory and application to simplex elements, *SIAM Journal on Scientific Computing* 38 (4) (2016) A1935–A1958.
- [7] R. M. Kirby, G. E. Karniadakis, De-aliasing on non-uniform grids: algorithms and applications, *Journal of Computational Physics* 191 (1) (2003) 249–264.
- [8] P.-O. Persson, J. Bonet, J. Peraire, Discontinuous Galerkin solution of the Navier–Stokes equations on deformable domains, *Computer Methods in Applied Mechanics and Engineering* 198 (17) (2009) 1585–1595.

- [9] D. M. Williams, An analysis of discontinuous Galerkin methods for the compressible Euler equations: entropy and L_2 stability, *Numerische Mathematik* 141 (4) (2019) 1079–1120.
- [10] Z. A. Worku, J. E. Hicken, D. W. Zingg, Very high-order symmetric positive-interior quadrature rules on triangles and tetrahedra, *J. Comput. Appl. Math.* 472 (C) (2026).
- [11] G. Chuluunbaatar, O. Chuluunbaatar, A. A. Gusev, S. I. Vinitsky, PI-type fully symmetric quadrature rules on the 3-, 6-simplexes, *Computers and Mathematics with Applications* 124 (2022) 89–97.
- [12] J. Jaśkowiec, N. Sukumar, High-order symmetric cubature rules for tetrahedra and pyramids, *International Journal for Numerical Methods in Engineering* 122 (1) (2021) 148–171.
- [13] S. Wandzurat, H. Xiao, Symmetric quadrature rules on a triangle, *Computers & Mathematics with Applications* 45 (12) (2003) 1829–1840.
- [14] Z. A. Worku, J. E. Hicken, D. W. Zingg, Quadrature rules on triangles and tetrahedra for multidimensional summation-by-parts operators, *Journal of Scientific Computing* 101 (1) (2024) 24.
- [15] F. Witherden, P. Vincent, On the identification of symmetric quadrature rules for finite element methods, *Computers & Mathematics with Applications* 69 (10) (2015) 1232–1241.
- [16] J. Jaśkowiec, N. Sukumar, Addendum to the paper “High-order symmetric cubature rules for tetrahedra and pyramids”, *International Journal for Numerical Methods in Engineering* 122 (7) (2021) 1875–1883.
- [17] A. Slobodkins, J. Tausch, A node elimination algorithm for cubature of high-dimensional polytopes, *Computers & Mathematics with Applications* 144 (2023) 229–236.
- [18] H. Xiao, Z. Gimbutas, A numerical algorithm for the construction of efficient quadrature rules in two and higher dimensions, *Computers & Mathematics with Applications* 59 (2) (2010) 663–676.
- [19] M. Festa, A. Sommariva, Computing almost minimal formulas on the square, *Journal of Computational and Applied Mathematics* 236 (17) (2012) 4296–4302.

- [20] E. J. Kubatko, B. A. Yeager, A. L. Maggi, New computationally efficient quadrature formulas for triangular prism elements, *Computers & Fluids* 73 (2013) 187–201.
- [21] M. G. Duffy, Quadrature over a pyramid or cube of integrands with a singularity at a vertex, *SIAM Journal on Numerical Analysis* 19 (6) (1982) 1260–1262.